



저작자표시-비영리-변경금지 2.0 대한민국

이용자는 아래의 조건을 따르는 경우에 한하여 자유롭게

- 이 저작물을 복제, 배포, 전송, 전시, 공연 및 방송할 수 있습니다.

다음과 같은 조건을 따라야 합니다:



저작자표시. 귀하는 원저작자를 표시하여야 합니다.



비영리. 귀하는 이 저작물을 영리 목적으로 이용할 수 없습니다.



변경금지. 귀하는 이 저작물을 개작, 변형 또는 가공할 수 없습니다.

- 귀하는, 이 저작물의 재이용이나 배포의 경우, 이 저작물에 적용된 이용허락조건을 명확하게 나타내어야 합니다.
- 저작권자로부터 별도의 허가를 받으면 이러한 조건들은 적용되지 않습니다.

저작권법에 따른 이용자의 권리는 위의 내용에 의하여 영향을 받지 않습니다.

이것은 [이용허락규약\(Legal Code\)](#)을 이해하기 쉽게 요약한 것입니다.

[Disclaimer](#)

공학석사 학위논문

**Observation of Ferroelectric
Critical Thickness of BaTiO₃ Thin
Film by Cs-corrected STEM**

구면수차보정 투과전자현미경을 이용한 BaTiO₃
산화물 박막의 강유전성 임계두께 관찰 연구

2018년 8월

서울대학교 대학원

재료공학부

김윤구

Abstract

Observation of Ferroelectric Critical Thickness of BaTiO₃ Thin Film by Cs-corrected STEM

Yoonkoo Kim

Department of Materials Science and Engineering

College of Engineering

Seoul National University

BaTiO₃ is well known for its ferroelectricity. However, its ferroelectricity can be changed under various external conditions. Particularly, the critical thickness that retains ferroelectricity have attracted continuous attention. Thus, it is very important to reveal critical elements that determine the ferroelectricity of BaTiO₃ in thin film structure to apply BaTiO₃ for electronic devices. In this study, we investigate the possibility of reducing the critical thickness of BaTiO₃ of 3.5 unit cell by introducing dielectric

SrTiO₃ layers, for which, 1unit cell and 10unit cell of SrTiO₃ on 2.5unit cell BaTiO₃ between SrRuO₃ electrodes are compared. Using high-resolution HAADF-STEM imaging, we measured displacements of cations to examine the existence of ferroelectricity for each samples. We extracted atomic peak positions from HAADF-STEM images and calculated ionic displacements of B cations (Ti, Ru), δ_{A-B} . From this δ_{A-B} , we found that there is ferroelectricity in 1unit cell SrTiO₃ sample, however, ferroelectricity disappears 10 unit cell SrTiO₃ sample. Ferroelectricity in 1 unit cell SrTiO₃ sample was also measured in piezoresponce force microscopy. This difference could be originated from theoretically expected, polarization penetration into electrodes. This result demonstrates that the thickness of the dielectric SrTiO₃ layer on BaTiO₃ can affect the critical thickness of BaTiO₃ ferroelectricity.

Keywords: Ferroelectricity, ionic polarization, Cs-corrected STEM, Piezoresponce Force Microscopy, BaTiO₃ thin film

Student Number: 2015-20810

Contents

Abstracts

Chapter 1 Introduction	1
Chapter 2 Literature Studies	3
2.1 BaTiO ₃ and its Ferroelectricity	3
2.2 Studies on BaTiO ₃ thin film structure	5
2.2 Critical Thickness in FE/Dielectric/Metal structure	16
Chapter 3 Experimental Details	18
3.1 Growth and Characterization of BaTiO ₃ films	18
3.2 Cs-corrected STEM observation and analysis.....	19
3.2 Piezoresponce Force Microscopy(PFM).....	20
Chapter 4 Resuluts and Discussion	22
4.1 Growth and Characterization of BaTiO ₃ films	22
4.2 Cs-corrected STEM observation and analysis.....	24
4.2.1 1u.c. SrTiO ₃ on 2.5u.c BaTiO ₃	24
4.2.2 10u.c SrTiO ₃ on 2.5u.c BaTiO ₃	31
4.3 Piezoresponce Force Microscopy(PFM).....	36
Chapter 5 Conclusion	37
References	39
Abstracts(Korean)	41

List of Figures

Figure 1	Schematic description of tetragonal ABO ₃ ferroelectric materials and ionic displacements.	4
Figure 2	Schematic description of bound charges in ferroelectrics and depolarization field.....	7
Figure 3	First-principle calculated ferroelectric displacements in SrRuO ₃ /BaTiO ₃ /SrRuO ₃ heterostructure.....	8
Figure 4	Schematic description for (a) asymmetric Ru and Ti termination layers and (b) symmetric Ti termination layers.	11
Figure 5	Energetic stability of ferroelectricity of BaTiO ₃ thin film according to film thickness and symmetry of termination layers .	12
Figure 6	(a) HAADF image of 3.5u.c BaTiO ₃ between SrRuO ₃ electrodes, (b) same sample with more magnified image, (c) intensity profile of long, diagonal white box in (b), (d) much more magnified image in white dashed box in (b) and atomic model	14
Figure 7	(a) HAADF image of 3.5u.c BaTiO ₃ between SrRuO ₃ electrodes, (b) plot of B site cation displacements.	15
Figure 8	(a) HAADF image of Si/SiO ₂ /SrTiO ₃ /BaTiO ₃ heterostructure, (b),(c) PFM amplitude and phase of Si/SiO ₂ /SrTiO ₃ /BaTiO ₃	17

Figure 9	Schematic description of our heterostructures. (a) 1u.c SrTiO ₃ /2.5u.c BaTiO ₃ and (b) 10u.c SrTiO ₃ /2.5u.c BaTiO ₃ between SrRuO ₃ electrodes.....	19
Figure 10	(a) AFM imaging of film heterostructure, (b) HRXRD 2θ-ω scan data.	23
Figure 11	(a) HAADF image with low magnification, (b) FFT image of HAADF image of 1u.c SrTiO ₃ on 2.5u.c BaTiO ₃	25
Figure 12	(a) HAADF image of 1u.c SrTiO ₃ on 2.5u.c BaTiO ₃ with high magnification, (b) intensity profile of long, red box region.	26
Figure 13	(a) HAADF image and integrated EDS signal mapping, (b)~(e) Each elemental maps for Ba, Ru, Ti and Sr in 1u.c SrTiO ₃ on 2.5u.c BaTiO ₃ respectively.	28
Figure 14	(a) Ferroelectric displacements, (b) c/a ratio in 1u.c SrTiO ₃ and 2.5u.c BaTiO ₃	30
Figure 15	(a) HAADF image with low magnification, (b) FFT image of HAADF image of 10u.c SrTiO ₃ on 2.5u.c BaTiO ₃	32
Figure 16	(a) HAADF image of 10u.c SrTiO ₃ on 2.5u.c BaTiO ₃ with high magnification, (b) intensity profile of red box region.	33
Figure 17	(a) HAADF image and integrated elemental signal mapping, (b)~(e) Each elemental maps for Ba, Ru, Ti and Sr in of 10u.c SrTiO ₃ on 2.5u.c BaTiO ₃ respectively.	34
Figure 18	(a) Ferroelectric displacements, (b) c/a ratio in 10u.c	

SrTiO₃ and 2.5u.c BaTiO₃. 35

Figure 19 PFM result for 1u.c SrTiO₃ on 2.5u.c BaTiO₃. 10

Chapter 1. Introduction

Perovskite transition metal oxide heterostructures have attracted extensive research interests because these oxide materials show various novel properties.¹ Especially, BaTiO₃ is one of the typical example of transition metal oxide which show strong ferroelectricity due to its simultaneous ionic polarization and have large dielectric constants compared to other various paraelectric and ferroelectric oxide materials.² Because of this high dielectric constant, Barium titanate is promising candidate material for many electronic devices such as capacitor, non-volatile memory (FeRAM) and piezoelectric actuator.³⁻⁵

Ferroelectric perovskite oxide materials like BaTiO₃ show their ferroelectricity as its unit cell structure changes.⁶ As described in Fig. 1, ions moves from their original position and these displacements generates polarization and ferroelectricity. This polarization makes BaTiO₃ have strong ferroelectricity. However, its ferroelectricity depends on many factors such as stoichiometry, crystal morphology, growth methodology and so on.²

Many researchers have interested in the ferroelectricity of BaTiO₃ in its thin film form. Because thin film structure is very general in device fabrication and attracts much industrial interests. Especially, ferroelectricity in oxide thin films degrade when the film thickness going thinner and interesting physical issues such as depolarization field and polarization penetration are related to here.⁷ We will talk about these issues later.

Because of these reasons mentioned, researchers performed many studies to find ferroelectric critical thickness of BaTiO₃ thin film sandwiched in two metal electrodes, especially SrRuO₃ or Pt.⁷⁻⁸ However, there were relatively small number of researches for BaTiO₃ thin film attached to dielectric material such as SrTiO₃.^{2,9} Ferroelectricity of BaTiO₃ on the dielectric material is quite important problem in the viewpoint of industry. Because most of practical electric devices use Si for substrate and Si substrate require dielectric buffer layer to grow ferroelectrics like BaTiO₃ on top of that.

In this paper, we grow BaTiO₃/SrTiO₃ thin film between SrRuO₃ electrodes to reproduce metal/dielectric/ferroelectric heterostructure and we performed Cs-corrected STEM observation using high angle annular dark field imaging to directly observe its ferroelectricity with varying thickness of dielectric layer, that is, SrTiO₃. Also we performed piezoresponce force microscopy to crosscheck the swiching property of ferroelectricity.

Here, we demonstrate that extremely thin BaTiO₃ thin film can show ferroelectricity with sufficiently thin dielectric SrTiO₃ thin film. However, when dielectric SrTiO₃ goes thicker, this ferroelectricity cannot be stabilized and disappear. We think that this phenomenon can occur because of polarization penetration into dielectric layer.

Chapter 2. Literature Studies

2.1 BaTiO₃ and Its Ferroelectricity

BaTiO₃ is a typical example of ferroelectric transition metal oxide. Among many oxide materials, BaTiO₃ attracts much research interest because of its strong dielectric constant and moderate Curie temperature (~120 °C).⁶ As known before, BaTiO₃ have much higher dielectric constant compared to many other materials such as PbZrO₃.² The origin of this strong dielectric constant is change of lattice constants. Paraelectric BaTiO₃ have cubic unit cell, however, ferroelectric BaTiO₃ have tetragonal unit cell in which Ti cation and oxygen anion move from its body center and face centers respectively.¹⁰ These ionic displacements generate ionic polarization. The schematic description of these ionic displacements are shown in Fig. 1. This strong polarization effect makes BaTiO₃ promising candidate material for various device applications such as field effect transistor, non-volatile memory.¹

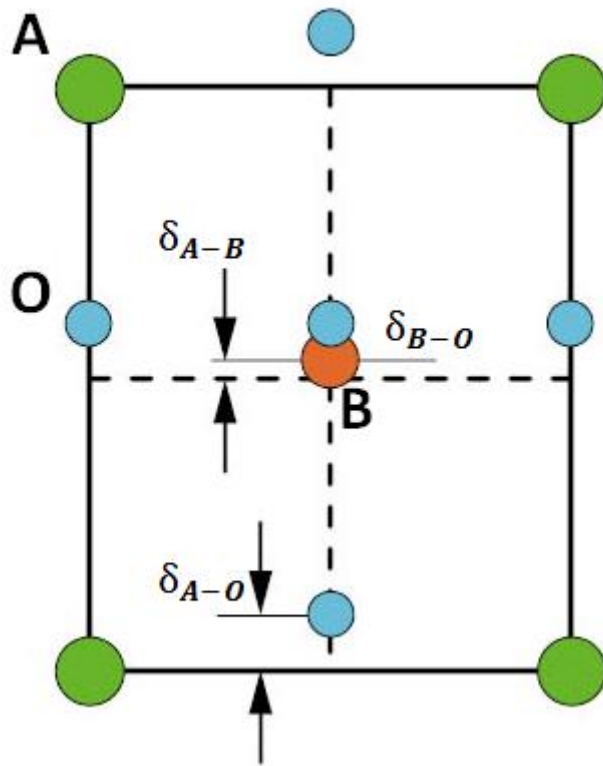


Figure 1 Schematic description of tetragonal ABO_3 ferroelectric materials and ionic displacements.

2.2 Studies on BaTiO₃ thin film heterostructure

As we mentioned, tetragonal BaTiO₃ has strong ferroelectricity. The electrical properties like ferroelectricity are affected by many factors such as chemical composition, crystal morphology.² Even fabrication method can affect to the ferroelectricity. Especially, because of continuing miniaturization of electric devices, stabilization of ferroelectric polarization at the nanometer scale become more and more important. Moreover, atomic scale growth techniques have advanced significantly recently, ones are able to control the number of unit cell, stacking sequence of nanometer scale oxide thin film. Therefore, many researchers have interests in the critical thickness of ferroelectricity of BaTiO₃ thin film.

Even though miniaturization tendency makes possible achieve high electric fields from low-voltage, but it also generates size effect and following degradation phenomena.¹² That is, the ferroelectricity of BaTiO₃ thin film going unstable as its thickness being thinner.

In general, there are two kind of explanations for this size effect. The first one is related to the free charges in the electrodes. As described in Fig. 2, because of polarization in the ferroelectric, free charges in electrodes approach to the interface to screen the electric field due to bound charges. This accumulated free charges generate new electric field which direction is opposite to the original electric field. This is called depolarization field which is described red arrow in Fig. 2.

This phenomenon is also known as Thomas-Fermi screening.¹³ Based on this depolarization field theory, Junquera et al studied ferroelectric critical thickness of SrRuO₃/BaTiO₃/SrRuO₃ thin film heterostructure.⁸ Using first-principle calculation, they calculated stability of ferroelectric polarization as a function of various BaTiO₃ thicknesses. From their calculation, Junquera et al found that until four unit cell, ferroelectricity in BaTiO₃ can be stabilized.

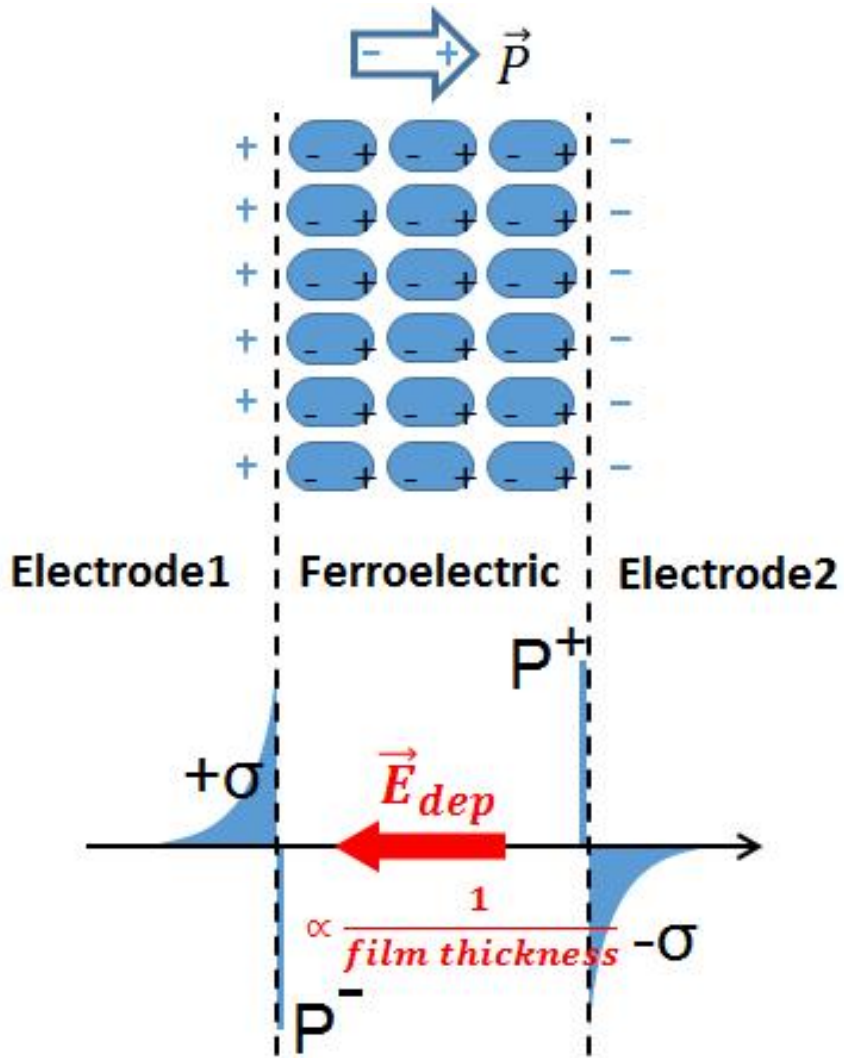


Figure 2 Schematic description of bound charges in ferroelectrics and depolarization field.

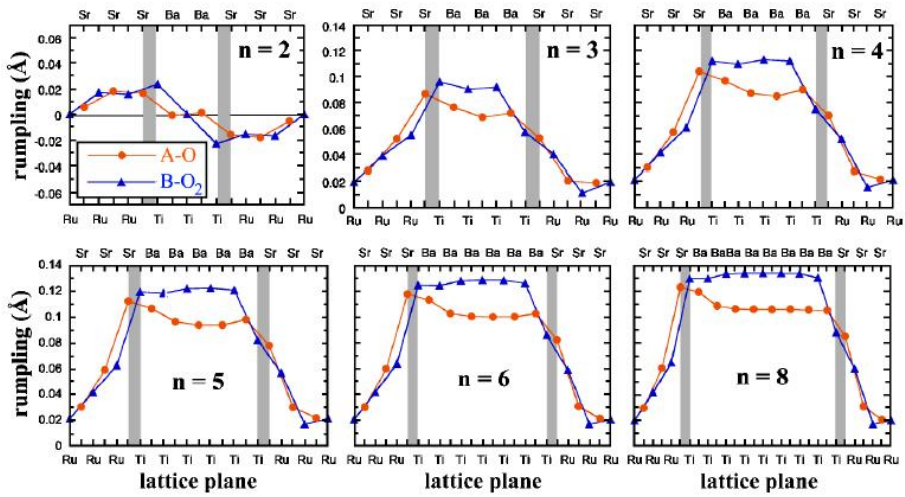


Figure 3 First-principle calculated ferroelectric displacements in SrRuO₃/BaTiO₃/SrRuO₃ heterostructure.⁷

The second explanation for the size effect is continuity effect. The polarization can't drop abruptly at the ferroelectric-electrode interface. Thus small polarization can exist in the electrode region. This is so-called Kretschmer-Binder effect.¹⁴ Gerra et al also performed first-principle calculation study to investigate the effect of this ferroelectric polarization penetration into the electrodes.⁷ They also used SrRuO₃/BaTiO₃/SrRuO₃ heterostructure with various BaTiO₃ thicknesses. For their calculation, they considered not only free charges but also ionic relaxation in the SrRuO₃ electrodes. Under these conditions, they found that 3.5u.c BaTiO₃ can show stable ferroelectric displacements as described in Fig. 3. In the Fig. 3, we can notice that there are stable ferroelectric displacements larger than 10pm in 3.5unit cell and more thick BaTiO₃ samples. However, in 2.5u.c samples, the magnitude of ferroelectric displacements in 2.5u.c BaTiO₃ is very small. This result implies that ferroelectric polarization can be stabilized till 3.5u.c BaTiO₃ thin film which have thinner thickness compared to result of Junquera et al.⁷⁻⁸

There is another issue for the ferroelectricity of BaTiO₃ thin film. The stacking sequence of the thin film is that. In the Fig. 4, there are two cases of SrRuO₃/BaTiO₃/SrRuO₃ thin film heterostructure. Both of Fig. 4(a) and (b) have three Ba layers between SrRuO₃ layers. However, at the top interfaces situation is different. Fig. 4(a) have Ru layer and Fig. 4(b) have Ti layer between Ba and Sr layers. These interfacial layers are called 'termination

layers' and Fig. 4(a) and (b) have different symmetry in their termination layers.

Lu et al studied the relation between these termination layers and ferroelectricity of BaTiO₃ thin film.¹⁵ They also performed first-principle calculation for SrRuO₃/BaTiO₃/SrRuO₃ heterostructure with varying BaTiO₃ thicknesses. However, to compare the effect of termination layer, they implemented one SrTiO₃ layer in one structure. Their structure and calculation results are shown in Fig. 5. A structure in Fig. 5(a) have asymmetric termination layers and Fig. 5(d) have symmetric termination layers. Other four figures show energetic stability of polarizations. Fig. 5(b) and (c) show that when BaTiO₃ have asymmetric termination layers, one of the two polarization direction is more stable than one another. However, when BaTiO₃ have symmetric termination layers, two polarization direction are all stable and makes ferroelectric swiching possible.¹⁵

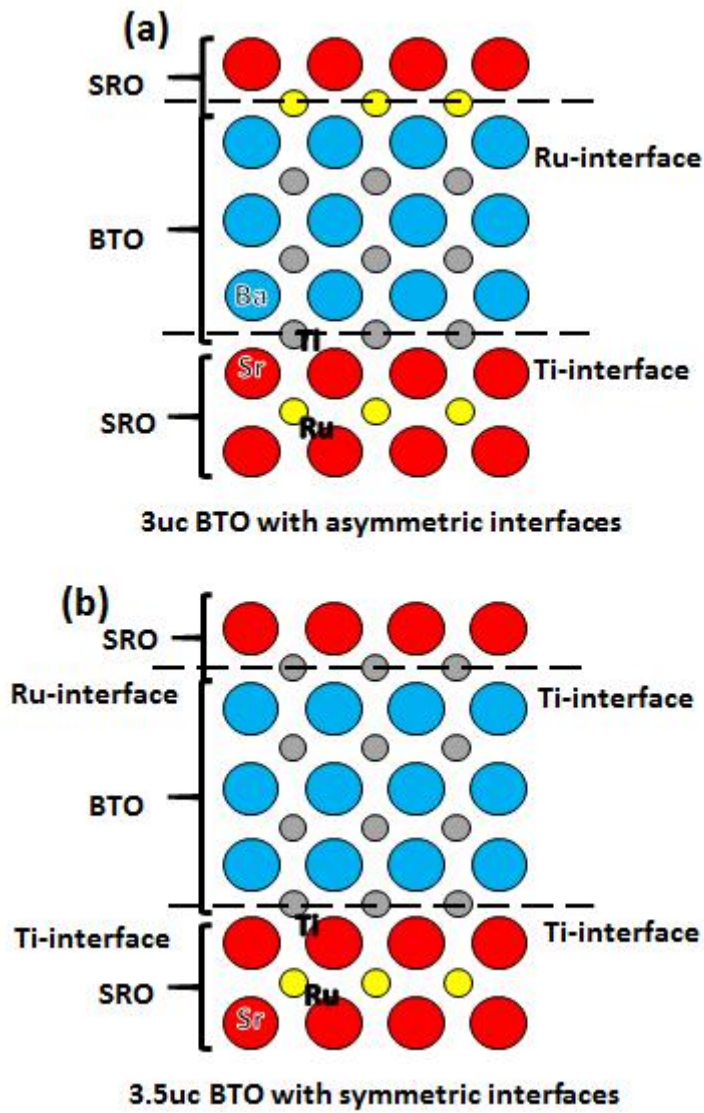


Figure 4 Schematic description for (a) asymmetric Ru and Ti termination layers and (b) symmetric Ti termination layers.

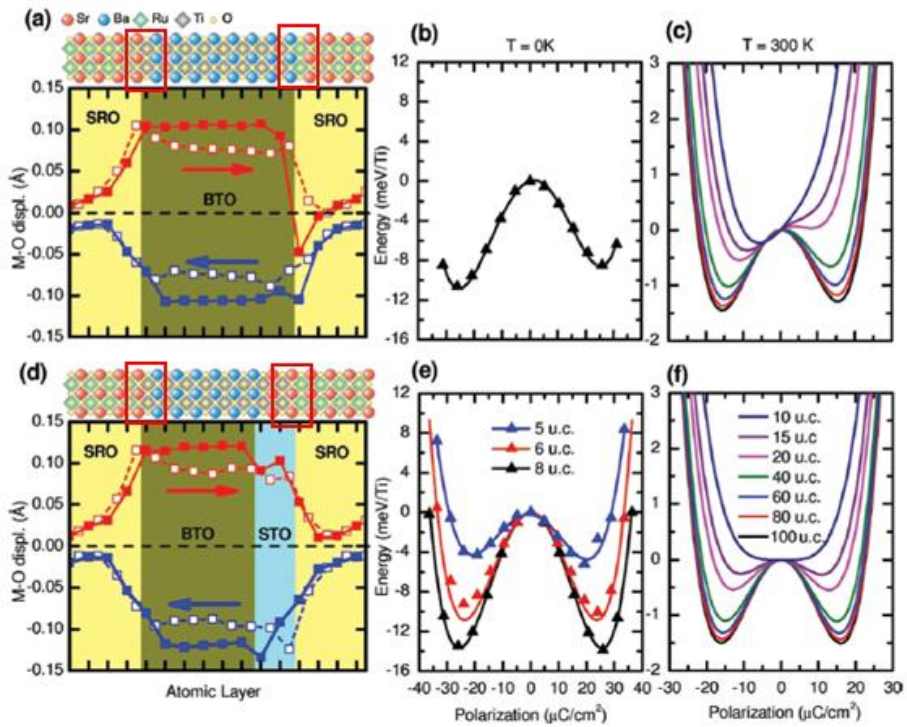


Figure 5 Energetic stability of ferroelectricity of BaTiO₃ thin film according to film thickness and symmetry of termination layers.¹⁵

The research of Lu et al show that symmetric termination layers are very important to embody switchable ferroelectricity. However, many studies on SrRuO₃/BaTiO₃/SrRuO₃ heterostructure have shown that atomic scale interface control is very difficult obstacle to approach theoretical limit, 3.5unit cell BaTiO₃.¹⁶⁻¹⁷ Shin et al succeeded in growth 3.5u.c BaTiO₃ between SrRuO₃ electrodes using pulsed laser deposition with atomically sharp symmetric Ti termination layers.¹¹ They controlled oxygen partial pressure and found that with low oxygen partial pressure condition Ti termination layer can be stabilized. Fig. 6 shows high angle annular dark field image of 3.5u.c BaTiO₃ heterostructure and we can observe that atomically sharp Ti termination layer in large region.

Fig. 7 shows Ti ionic displacements in 3.5u.c BaTiO₃ thin film. B cation displacement, δ_{A-B} in Fig. 1. The plot in Fig. 7(b) shows ferroelectric displacements of Ti cations and their penetration into SrRuO₃ electrode. These displacements are direct evidence of ferroelectric displacements in 3.5u.c BaTiO₃ thin film, that is, theoretical limit thickness of stable ferroelectricity in BaTiO₃ thin film structure.

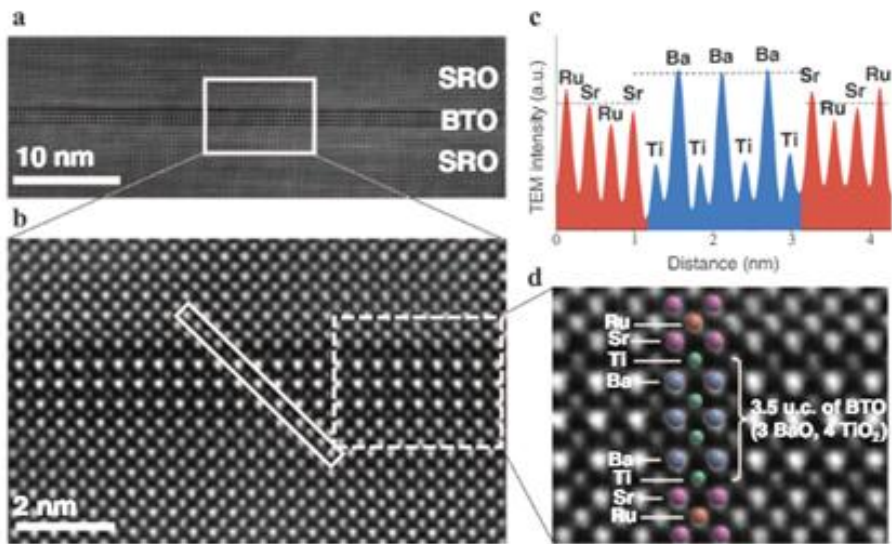


Figure 6 (a) HAADF image of 3.5u.c BaTiO₃ between SrRuO₃ electrodes, (b) same sample with more magnified image, (c) intensity profile of long, diagonal white box in (b), (d) much more magnified image in white dashed box in (b) and atomic model.¹¹

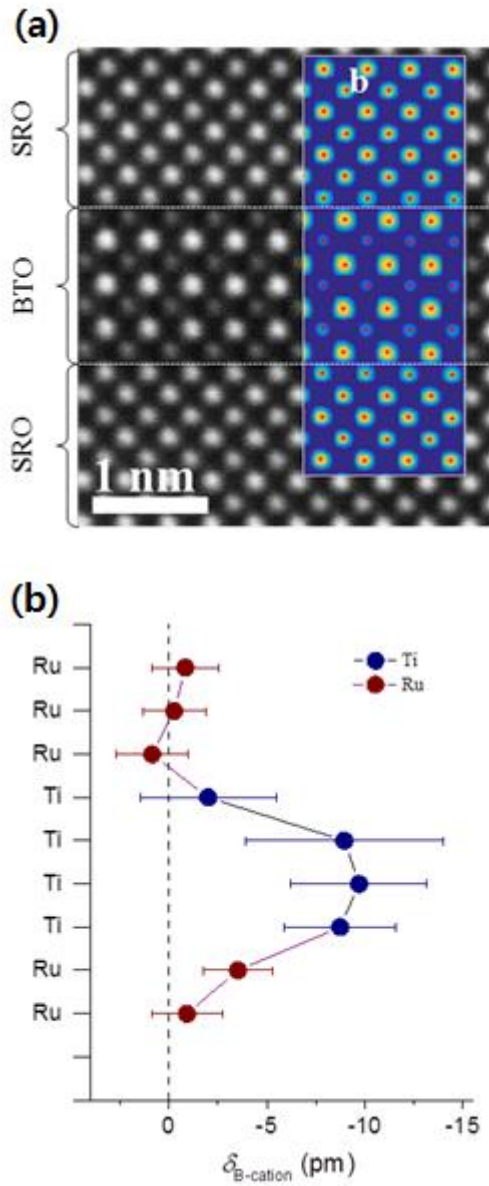


Figure 7 (a) HAADF image of 3.5u.c BaTiO₃ between SrRuO₃ electrodes, (b) plot of B site cation displacements.¹¹

2.3 Critical thickness of BaTiO₃ in FE/Dielectric structure

We introduced many researches dealing with critical thickness of ferroelectricity of BaTiO₃ thin film. However, all those researches required metallic SrRuO₃ electrodes. Of course, SrRuO₃/BaTiO₃/SrRuO₃ heterostructure is great model system to investigate ferroelectric critical thickness. However such metal/ferroelectric/metal structure is somewhat different from real device structure. In real industry, most of electric devices use Si substrate. It is very important issue to grow BaTiO₃ thin film on top of Si substrate directly.¹⁸ Therefore, one grow SrTiO₃ on the Si substrate first and then grow BaTiO₃ film on the SrTiO₃ film. In this Si/SrTiO₃/BaTiO₃ structure, doped Si have metallic property and SrTiO₃ is dielectric. Consequently, this structure has metal/dielectric/ferroelectric properties respectively. This is quite different compared to SrRuO₃/BaTiO₃/SrRuO₃ structure, which have metal/ferroelectric/metal properties.

Dubourdieu et al tried to grow mentioned thin film system.⁶ Fig. 8(a) shows high angle annular dark field image of Si/SiO₂/SrTiO₃/BaTiO₃ system. High resolution STEM image shows highly crystalline BaTiO₃ film can grow on SrTiO₃. Then how about the ferroelectricity of such system? To measure ferroelectricity in this metal/dielectric/ferroelectric structure, Dubourdieu et al and Mazet et al performed piezoresponce force microscopy(PFM).⁹ Fig. 8(b) and (c) shows PFM amplitude and phase

respectively. Fig. 8(b) shows typical ‘butterfly curve’ which implies the existence of ferroelectric switching.¹⁹ Such researches say that BaTiO₃ film on Si/SrTiO₃ can exhibit ferroelectricity. However, the critical thickness of ferroelectricity in these model system is unknown.

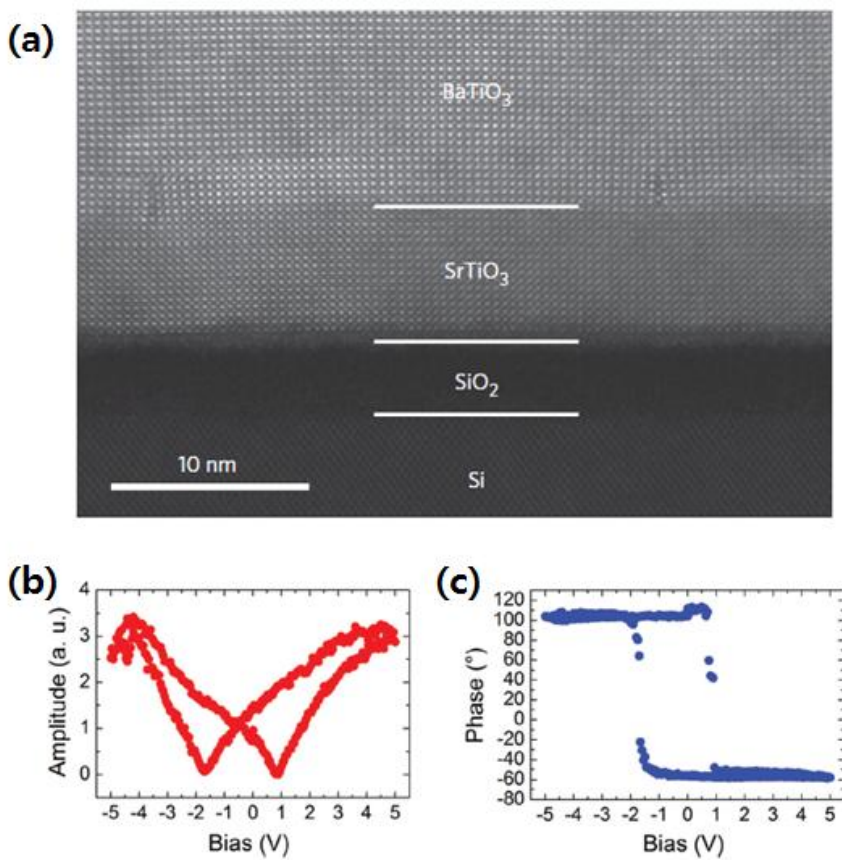


Figure 8 (a) HAADF image of Si/SiO₂/SrTiO₃/BaTiO₃ heterostructure, (b),(c) PFM amplitude and phase of Si/SiO₂/SrTiO₃/BaTiO₃^{6,9}

Chapter 3. Experimental Details

3.1 Growth and Characterization of BaTiO₃ films

Our perovskite thin films were fabricated by a pulsed laser deposition (PLD) system with a KrF excimer laser ($\lambda = 248\text{nm}$). Before deposition, SrTiO₃(001) substrates were etched using buffered hydrofluoric acid and annealed at 1000 °C in an ambient oxygen flow to create atomically smooth TiO₂-terminated surfaces. The temperature of the substrate was 700 during deposition and the laser fluence repetition rate were set at 1.5 J/cm² and 2 Hz, respectively. The SrRuO₃ electrodes were grown at an oxygen partial pressure (P_{O_2}) of 100 mTorr and ultrathin BaTiO₃ layers were subsequently deposited at $P_{\text{O}_2} = 5\text{mTorr}$. The heterostructures were ex-situ annealed at 600 in an ambient oxygen flow for 1 hour to minimize the oxygen deficiency.²⁰ Following above processes, two heterostructure films samples were fabricated. In the first sample, 20 nm SrRuO₃ bottom electrode was deposited on top of SrTiO₃ substrate. On the bottom electrode, 2.5 u.c BaTiO₃, 1 u.c SrTiO₃, 20 nm SrRuO₃ top electrode are deposited consecutively. For second sample, on top of 20 nm bottom electrode, 2.5 u.c BaTiO₃, 10 u.c SrTiO₃, 20 nm top electrode are deposited in the same manner. Schematic description of these two samples are given in Fig. 9.

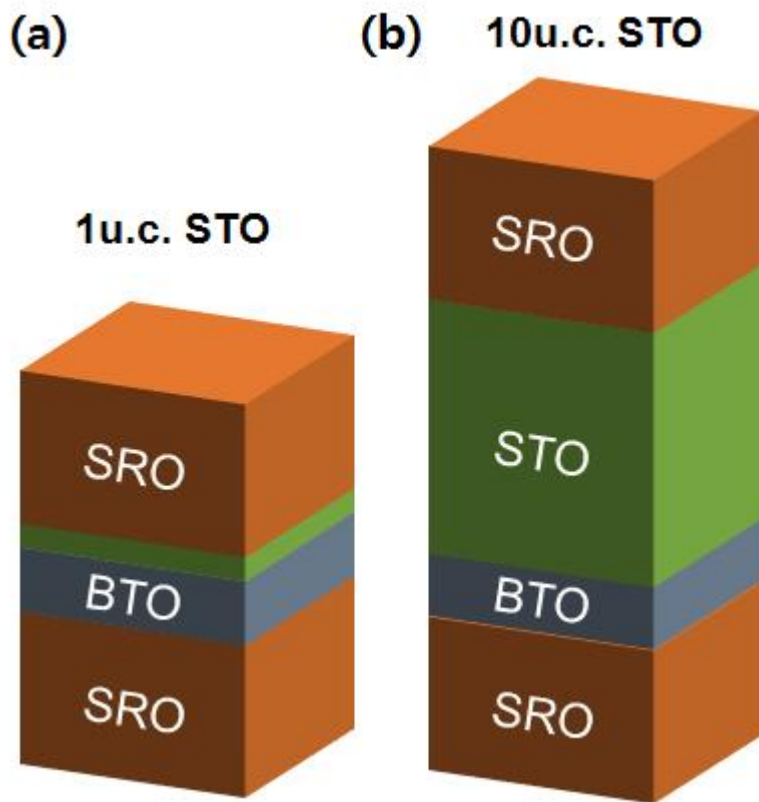


Figure 9 Schematic description of our heterostructures. (a) 1u.c $\text{SrTiO}_3/2.5\text{u.c BaTiO}_3$ and (b) 10u.c $\text{SrTiO}_3/2.5\text{u.c BaTiO}_3$ between SrRuO_3 electrodes.

High resolution XRD and atomic force microscopy(AFM) observations were followed after film fabrication processes to investigate surface morphology and crystalline quality of heterostructure film system.²⁰ AFM and XRD results are given in Fig. 10.

3.2 Cs-corrected STEM observation and analysis

After the film sample deposition, TEM specimens were made by focused ion beam(FIB). When sample prepared, fine milling is following using nanomill. Cs-corrected STEM observation was performed.

Cs-corrected STEM observation was performed by JEOL ARM-200F in National Center for Interuniversity Research Facility(NCIRF), Seoul National University. Acceleration voltage was 200kV. When we obtain high angle annular dark field image(HAADF), JEOL STEMMeister software integrated 30 images to correct sample drift effect.

Using HAADF images, we investigated peak position of each atomic columns by two dimensional fitting. For this, we used peak pairs analysis algorithm developed by Ishizuka et al.²¹

3.3 Piezoresponce Force Microscopy(PFM)

The swiching properties of ferroelectric ionic polarization were measured by an piezoresponce force microscopy using atomic force microscopy at room temperature. A Cr/Pt-coated probe tip with a 40N/m

spring constant and a resonant frequency of 400kHz was used. The high spring constant and contact resonance frequency minimized possible effects of nonpiezoelectric response, such as electrostatic force.¹¹

Chapter 4. Results and Discussion

4.1 Growth and Characterization of BaTiO₃ films

The characterization of two samples with different SrTiO₃ thickness described in Fig. 9 was performed by atomic force microscopy and high resolution XRD. Fig 10 below show AFM image and XRD scan of our heterostructure film system.

As shown in Fig 10(a), AFM image show typical step-terrace surface morphology. Its wide terrace regions show that SrRuO₃ top electrode have atomically smooth surface roughness under 1nm. Each terrace area is up to in hundreds nm region. It means that our film system have atomically flat structure in wide region.

Next, in Fig 10(b), HRXRD image show 2θ - ω scan result. It shows two major peaks which are SrTiO₃ (002) and SrRuO₃(220) respectively. High and sharp SrTiO₃ (002) peak come from SrTiO₃ substrate. SrRuO₃(220) peak show that SrRuO₃ electrodes are well stabilized on top of SrTiO₃ substrates. Because there were no any other major peaks, there were not other secondary phases in scanning range. Therefore, we confirmed that SrRuO₃ films were deposited on substrates epitaxially. We cannot observe XRD peak for BaTiO₃ because 2.5u.c BaTiO₃ layers are too thin to be measured in XRD scan. High crystallinity of our samples can be confirmed again in our high resolution STEM images.

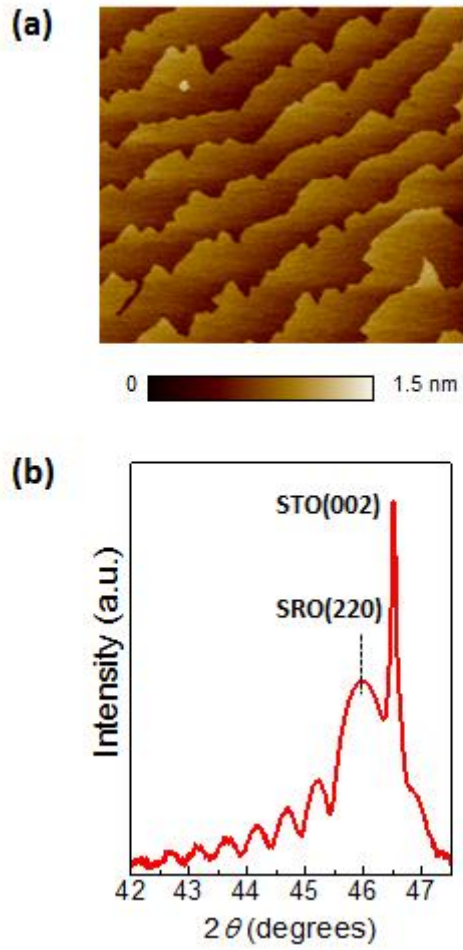


Figure 10 (a) AFM imaging of film heterostructure, (b) HRXRD 2θ - ω scan data.

4.2 Cs-corrected STEM observation and analysis

As described in Fig 9, we observed two samples with different SrTiO₃ thicknesses, 1u.c and 10u.c respectively. In this section, we will discuss Cs-corrected STEM observation images and analysis results for each samples.

4.2.1 1u.c SrTiO₃ on 2.5u.c BaTiO₃ films

Fig 11 shows the high resolution annular dark field image of our heterostructure film system of 1u.c SrTiO₃ on the 2.5u.c BaTiO₃ between two SrRuO₃ electrodes. Fast Fourier transform of HAADF image in Fig. 11(b) shows typical perovskite (100) zone axis and there are no any half-integer peaks which imply the existence of supercell structure. This result corresponds with the XRD result in Fig. 10 which shows no any other secondary phase of SrRuO₃ and BaTiO₃. It means that our SrRuO₃ and BaTiO₃ film structure deposited epitaxially on top of SrTiO₃ substrate and have stable pseudo-cubic structure.

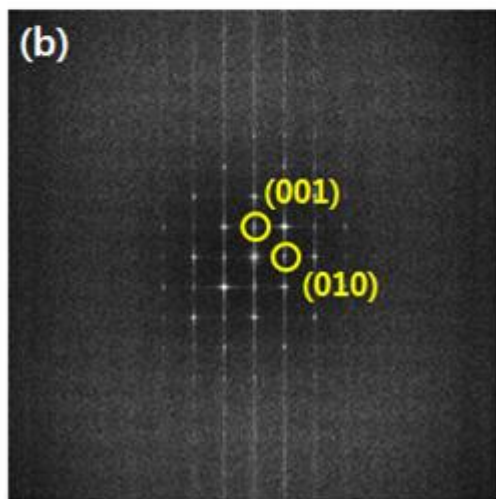


Figure 11 (a) HAADF image with low magnification, (b) FFT image of HAADF image of 1u.c SrTiO₃ on 2.5u.c BaTiO₃.

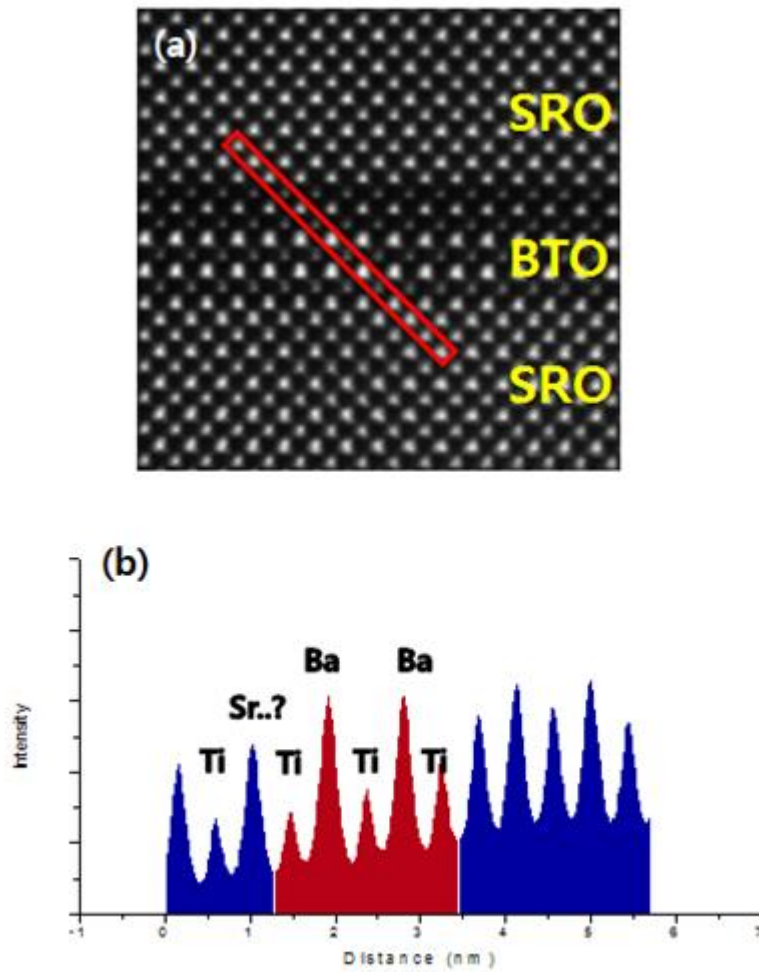


Figure 12 (a) HAADF image of 1u.c SrTiO₃ on 2.5u.c BaTiO₃ with high magnification, (b) intensity profile of long, red box region.

Fig. 12(a) is more magnified HAADF image of 1u.c SrTiO₃ and 2.5u.c BaTiO₃ sample. Between top and bottom SrRuO₃ electrodes, we can easily observe two A site cation layer and three B site cation layers. Even in bare eyes, we can see two A site cation layers are brighter than one other A site cation layer. Fig. 12(b) shows intensity line profile of red box in Fig. 12(a). we can see intensity peaks for each A and B site cations alternatively. We know (Sr and Ba) for A site and (Ru and Ti) for B site cations respectively. Therefore, among three A site cation peaks between SrRuO₃ electrodes, two peaks have higher intensities than one another peak. In HAADF STEM image, peak intensity is proportional to the square of atomic number[], so we can expect that this smaller peak is a Sr atomic column and other two peaks with higher intensities are Ba respectively.

To confirm the film structure and the existence of 1u.c SrTiO₃ layer between top electrode and 2.5u.c BaTiO₃, we performed energy dispersive spectroscopy(EDS) measurement for elemental analysis. Fig 13 shows two dimensional elemental mapping images. Fig. 13(e), that is, Sr elemental map apparently shows that there are one Sr layer on top of Ba layers. Therefore, we confirmed that one unit cell of SrTiO₃ layer between top SrRuO₃ electrode and BaTiO₃ thin film.

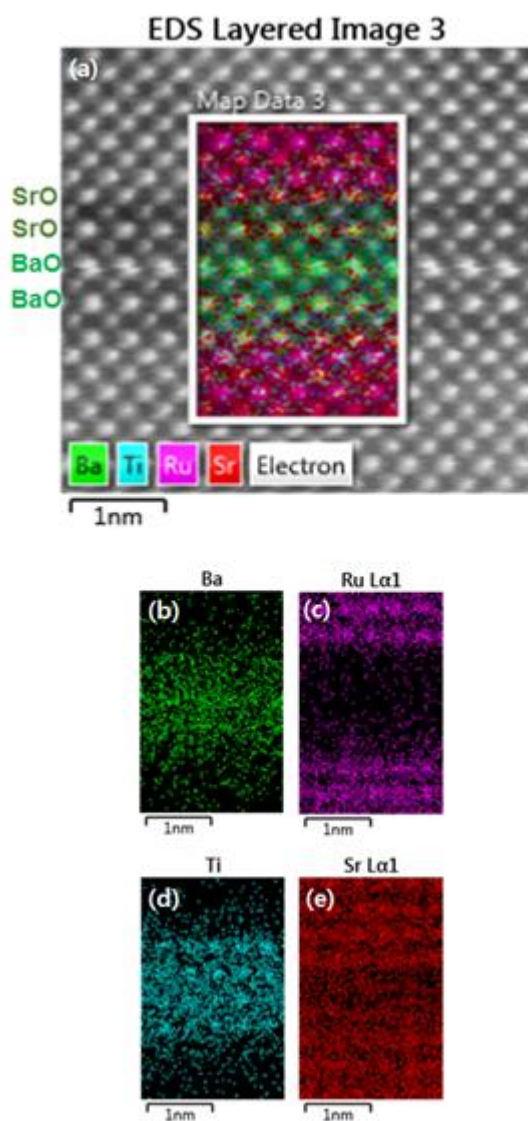


Figure 13 (a) HAADF image and integrated EDS signal mapping, (b)~(e) Each elemental maps for Ba, Ru, Ti and Sr in 1u.c SrTiO₃ on 2.5u.c BaTiO₃ respectively.

Next, to measure the ferroelectric displacement of B site cations in BaTiO₃ region, we measured atomic peak positions by two dimensional fitting of atomic columns. We used peak finding tool implemented in peak pairs algorithm software package developed by Ishizuka et al.²¹ As explained in Fig. 1, we calculated difference between real B site cation position and midpoint of four A site cation positions for each unit cell. Fig. 14 shows the result from this image analysis for 1u.c SrTiO₃ sample. As legend shows, red dots mean cation displacements of Ru ions. Green and blue dots mean Ti displacements. Especially, blue dots mean Ti displacements in 2.5u.c BaTiO₃ layers and green do mean Ti displacement in termination layer between SrRuO₃ electrode and SrTiO₃ layer. These four Ti layers show more than 10pm displacements, this is the direct evidence of ferroelectricity and polarization penetration expected in Gerra et al's study.⁷ Moreover, among many images, more than 70% of images (26 images from total 36 images) shown ferroelectric displacements like Fig. 14(a).

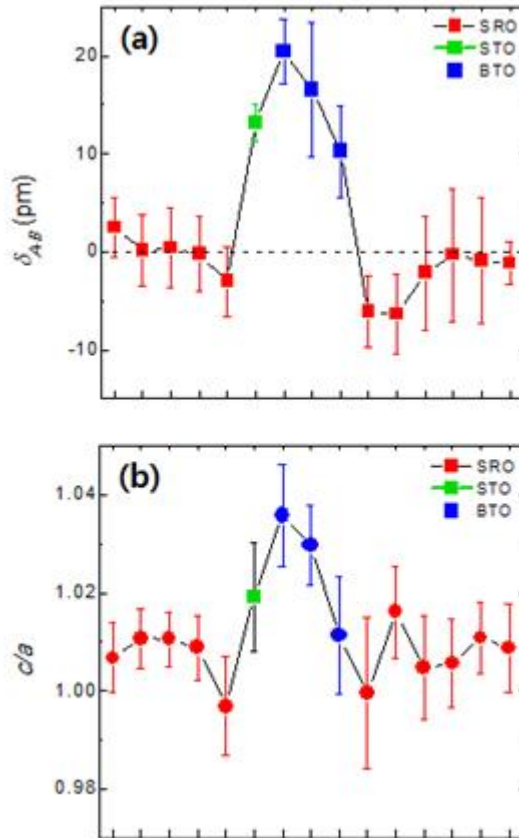


Figure 14 (a) Ferroelectric displacements, (b) c/a ratio in 1.u.c SrTiO_3 and 2.5.u.c BaTiO_3

4.2.2 10u.c SrTiO₃ on 2.5u.c BaTiO₃

Same as 1u.c SrTiO₃ on 2.5u.c BaTiO₃ sample, we observed 10u.c SrTiO₃ on 2.5u.c BaTiO₃ sample. Low magnification high angle annular field image and its fast fourier transform image are given in Fig 15. As shown in Fig 15(a), on Top of SrRuO₃ bottom electrode, 2.5u.c BaTiO₃, 10u.c SrTiO₃ and SrRuO₃ top electrode are deposited consecutively. Fig. 15(b), fast fourier transform image of Fig. 15(a) shows perovskite (100) zone axis same as Fig. 14(b). It implies that our 10u.c SrTiO₃ sample have epitaxial film structure similar with 1u.c SrTiO₃ sample.

Same as 1u.c SrTiO₃ sample, Fig. 16 shows magnified image of 10u.c SrTiO₃ on top of 2.5u.c BaTiO₃ film. We can observe two bright Ba layers below SrTiO₃ layer in the Fig 16(b), the intensity profile. Therefore, we can expect that there are only two Ba layers on top of bottom SrRuO₃ electrode. To confirm this, we performed EDS measurement for elemental mapping. Sr and Ti elemental maps, Fig. 17(d) and (e) show that SrTiO₃ exist on top of 2.5u.c BaTiO₃. It confirms that there are two Ba layers under the SrTiO₃ film.

Next, Fig. 18 shows ionic displacements and c/a ratio for 10u.c SrTiO₃ sample. In contrast to Fig. 14(a), 10u.c sample do not show any ionic displacements in all regions. It means that there is no ferroelectricity in this 10u.c SrTiO₃ and 2.5u.c BaTiO₃ sample. As we did for 1u.c. SrTiO₃ sample, we investigated many images and found that more than 70% of images (20 imgs from 27 images) do not have any sign of ferroelectricity. Especially,

the magnitude of Ti displacements was smaller than 5pm. Moreover, other 7 images, Ti cations move ~5pm in average. The pixel size of our STEM images is 6.505pm per pixel. Thus this 5 pm displacement is not meaningful and we can demonstrate that in the 5pm scale level, there are no displacements in 10u.c SrTiO₃ on 2.5u.c BaTiO₃ sample. Therefore, we concluded that in 10u.c SrTiO₃ sample, ferroelectric displacement is not stable and moreover, no polarization penetration exists.

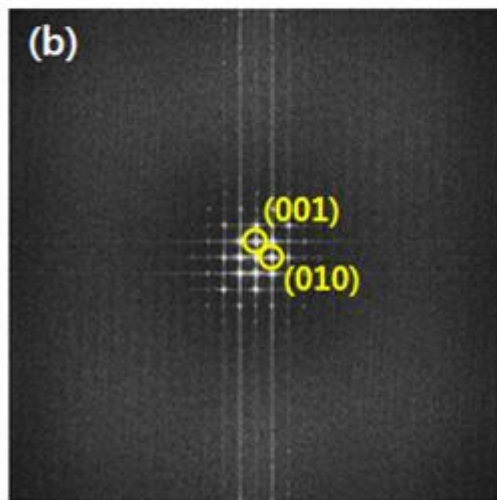
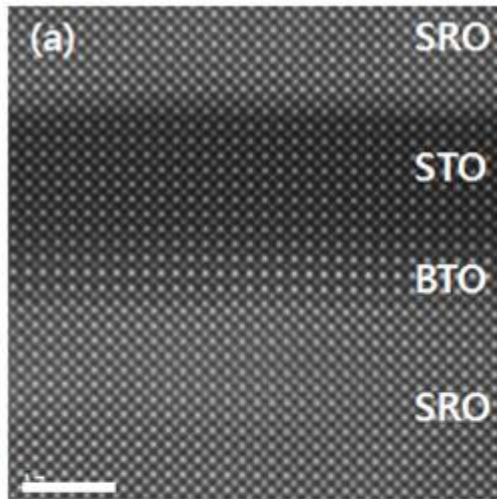


Figure 15 (a) HAADF image with low magnification, (b) FFT image of HAADF image of 10u.c SrTiO₃ on 2.5u.c BaTiO₃.

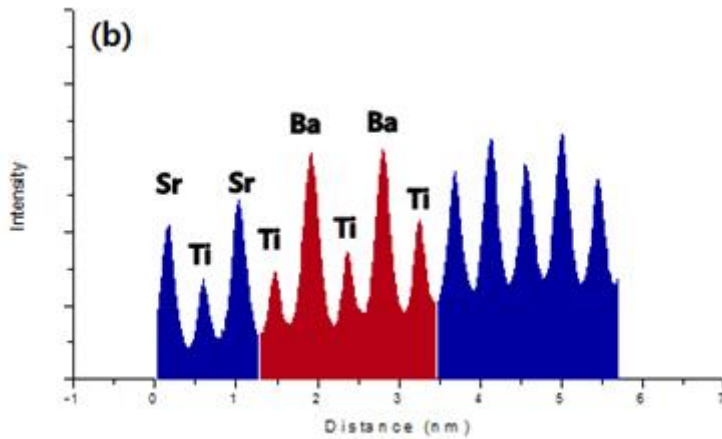
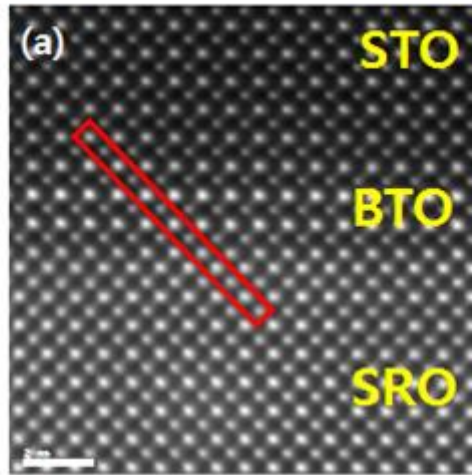


Figure 16 (a) HAADF image of 10u.c SrTiO₃ on 2.5u.c BaTiO₃ with high magnification, (b) intensity profile of red box region.

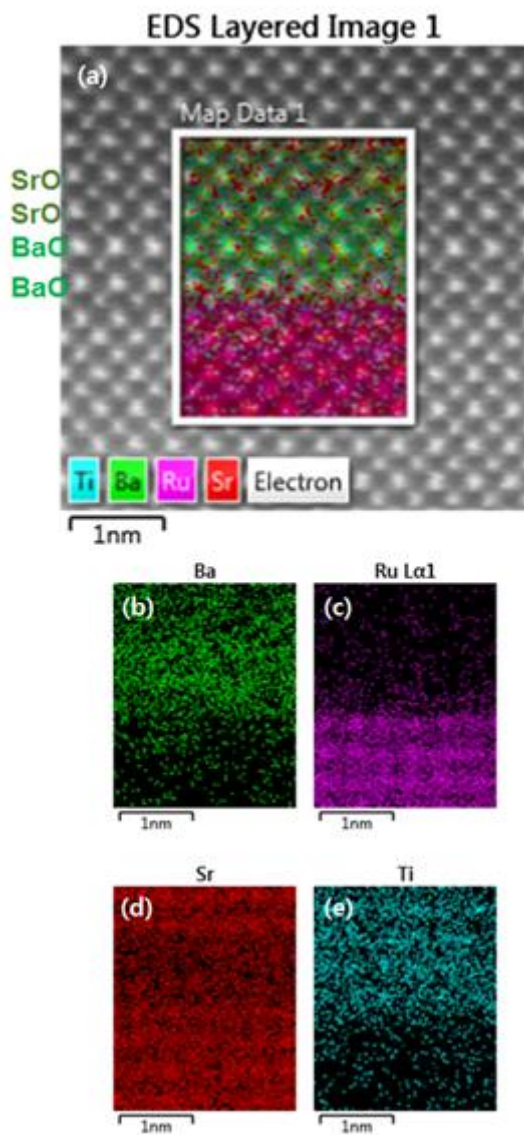


Figure 17 (a) HAADF image and integrated elemental signal mapping, (b)~(e) Each elemental maps for Ba, Ru, Ti and Sr in of 10u.c SrTiO₃ on 2.5u.c BaTiO₃ respectively.

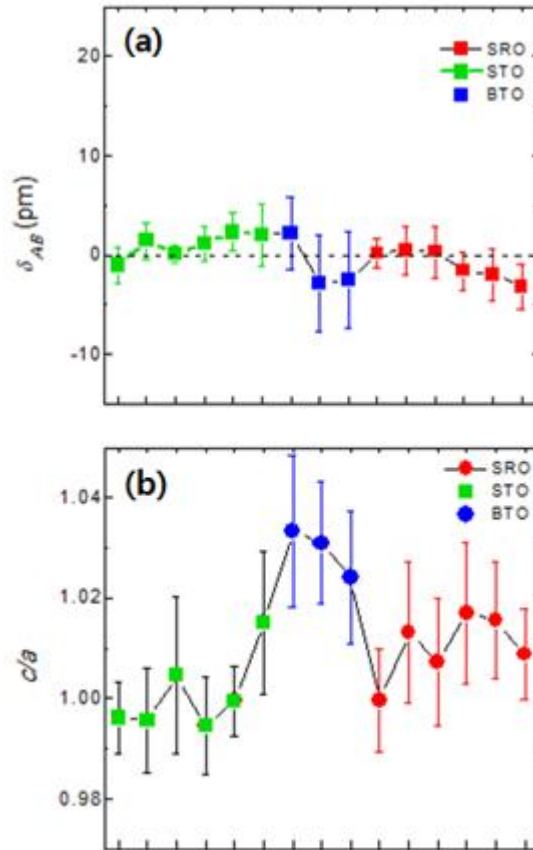


Figure 18 (a) Ferroelectric displacements, (b) c/a ratio in 10u.c SrTiO₃ and 2.5u.c BaTiO₃

4.3 Piezoresponse Force Microscopy(PFM)

PFM measures an expansion and contract of lattice constant using atomic force microscopy. If an oxide film had swichable ferroelectricity, PFM amplitude and phase should have butterfly curve and 180° phase difference respectively, as described in Fig. 19. Fig. 19 is experimental PFM result for 1u.c SrTiO₃ on 2.5u.c BaTiO₃ sample. Two vertical axis are PFM phase(left, blue) and amplitude(right, red) respectively. PFM amplitude shows apparent butterfly curve and 180° phase difference. This is another evidence of ferroelectricity correspond to the Ti displacements shown in Fig. 14(a).

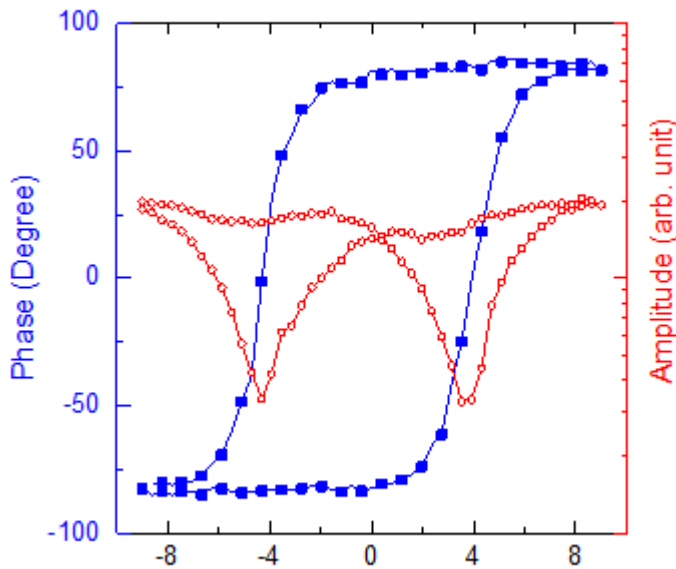


Figure 19 PFM result for 1u.c SrTiO₃ on 2.5u.c BaTiO₃.

Chapter 5. Conclusion

To investigate ferroelectric critical thickness of BaTiO₃ thin film in metal/dielectric/ferroelectric heterostructure, we observed two samples, 1u.c SrTiO₃ on 2.5u.c BaTiO₃ and 10u.c SrTiO₃ on 2.5u.c BaTiO₃ using high angle annular dark field imaging by Cs-corrected STEM and measured ionic displacements using peak position finding. Using this image processing technique, we calculated δ_{A-B} in Fig. 1 to observe ferroelectric ionic displacements.

In 1u.c SrTiO₃ on 2.5u.c BaTiO₃ sample, Ti cations show ferroelectric displacements as displayed in Fig. 14. This is direct evidence of Ferroelectricity. However in 10u.c SrTiO₃ on 2.5u.c BaTiO₃ sample, Ti cations do not show significant ferroelectric displacements. It means there are no spontaneous polarization in this sample.

We also performed PFM measurement for 1u.c SrTiO₃ on 2.5u.c BaTiO₃. PFM amplitude and phase show typical butterfly curve and hysteresis like loop. These curves are general in ferroelectric materials. Thus PFM result also supports the stable ferroelectricity in 1u.c SrTiO₃ on 2.5u.c BaTiO₃ structure.

We think that this stable ferroelectric polarization in 2.5u.c BaTiO₃ is closely related with 1u.c SrTiO₃ layer. Like Gerra et al's study,⁷ polarization

penetration into very thin SrTiO₃ may stabilize the polarization. However, unlike Gerra et al's result, polarization penetration in our sample is limited only one unit cell of SrTiO₃. In SrRuO₃ region, almost no polarization penetration was observed. Therefore, though we observed ferroelectric polarization in 1u.c SrTiO₃ on 2.5u.c BaTiO₃ heterostructure, much more studies including first-principle calculation are necessary to complete understanding of ferroelectricity in metal/dielectric/ferroelectric system.

References

- [1] M.B. Salamon et al., *Rev. Mod. Phys.* 73, 583(2001)
- [2] R. Ulrich et al., *The International Journal of Microcircuits and Electronic Packaging*, 23, 2, (2000)
- [3] J. F. Scott, *Ferroelectric Memories*, Springer, (2000)
- [4] O. Auciello et al., *Phys. Today* 51, No, 7, 22 (1998)
- [5] N. Setter, *Electroceramic-Based MEMS*, Springer (2005)
- [6] C. Dubourdieu et al., *Nature Nanotechnology*, 8, 748, (2013)
- [7] G. Gerra et al., *PRL*, 96, 107603 (2006)
- [8] J. Junquera et al., *Nature*, 422, 506, (2003)
- [9] L. Mazet et al., *J. Appl. Phys.* 116, 214102 (2014)
- [10] C.L. Jia et al., *Nature Materials* 6, 64 (2007)
- [11] Y.J Shin et al., *Adv. Mater*, 29, 1602795 (2017)
- [12] A. K. Tagantsev, *J. Appl. Phys.* 90, 1387 (2001)
- [13] R. D. Tilley et al., *Ferroelectrics*, 134, 313 (1992)
- [14] R. Kretschmer et al., *phys. Rev. B*, 20, 1065 (1979)
- [15] H. Lu et al., *Adv. Mater.* 24, 1209 (2012)
- [16] J. Shin et al., *ACS Nano*, 4, 4190, (2010)
- [17] G. Rijnders et al., *Appl. Phys. Lett.* 84, 505 (2004)
- [18] S. Salahuddin et al., *NaNo let*, 8, 405 (2008)

[19] www.ntmdt-si.com/resources/applications/piezoresponse-force-microscopy-in-its-applications

[20] L. Wang et al., *Adv. Mater.*, 29, 1802001 (2017)

[21] P.L. Galindo et al., *Ultramicroscopy*, 107, 1186 (2007)

초 록

BaTiO₃는 특유의 강유전성으로 인해 주목받고 있는 물질이지만 그 강유전성은 다양한 외부 조건들로 인해 크게 변화할 수 있다. 따라서 실제 소자에서 널리 사용되는 박막 구조로 제작되었을 때 어떤 메커니즘이 BaTiO₃의 강유전성에 영향을 미치는지를 이해하는 것은 BaTiO₃를 이해하고 실제 소자에 적용하기 위해 필수적이라 할 수 있다. 본 연구에서 우리는 SrRuO₃ 전극과 2.5 유닛 셀의 극히 얇은 BaTiO₃ 박막 사이에 각각 1유닛 셀과 10유닛 셀 두께의 SrTiO₃ 층을 갖는 박막 구조 샘플들을 제작하였고 고배율 HAADF-STEM 이미징 기법을 사용하여 원자 수준에서 양이온들의 움직임을 측정, 각각의 샘플에서의 강유전성의 유무를 관찰하였다. HAADF-STEM 이미지에서 얻은 원자 피크 위치 정보로부터 B 위치 양이온(Ru, Ti)들의 위치 변화량인 δ_{A-B} 값을 계산할 수 있었고 이로부터 1유닛 셀 두께의 SrTiO₃를 가지는 BaTiO₃ 샘플에서 강유전성이 관찰되지만, 10유닛 셀 SrTiO₃ 샘플에서는 강유전성이 관찰되지 않음을 확인하였다. 이러한 차이는 이론적으로 예측된, 이온 분극이 전극 안으로 뚫고 들어가는 현상으로 설명될 수 있다. 또한 1유닛 셀 SrTiO₃ 샘플에서의 강유전성은 압전현미경 실험 결과와 일치하였다. 본 연구로부터 SrTiO₃와 같은 유전체의 두께가 강유전성 임계 두께에 영향을 줄 수 있음을 확인할 수 있다.

주요어: 강유전성, 이온 분극, 구면수차보정 주사투과전자현미경,

압전현미경, BaTiO₃ 박막
학 번: 2015-20810

Observation of Ferroelectric Critical

Thickness of BaTiO₃ Thin Film by 2018 김윤구

Cs-corrected STEM



